Turbulent Drag Reduction and Phase Behavior of a Mixed Zwitterionic and Cationic Surfactant Solution Exhibiting Dilution Precipitation

Christopher M. Poore

November 30, 2016

Contents

1 Abstract

A drag reducing fluid consisting of a zwitterionic and cationic surfactant with an added counterion was observed to exhibit interesting phase behavior. At equimolar surfactant concentrations, dilution precipitation was observed. It was later noted that this system also exhibits shear precipitation. Phase diagrams were constructed to better understand the conditions under which this behavior occurs. Drag reduction data were collected using a recirculating flow system to evaluate drag reducing effectiveness. Further tests were performed using an Ares Rheometer to evaluate how the first normal stress difference is affected by the phase change. Attempts were made to quantify and describe the precipitate composition using infrared spectroscopy.

2 Introduction and Background

2.1 History of Drag Reduction

Turbulent drag reduction is a unique turbulent flow phenomenon that occurs when a small amount of additive is present in a carrier fluid[1]. The result is a drastic reduction in turbulent friction loss. As a result, a much smaller pressure drop is observed and pumping requirements are lessened. What makes this phenomenon so interesting is that the flow is still turbulent, however the structure of the flow is modified. This was first observed in 1931 by Forrest and Grierson when studying wood-pulp fiber suspensions in water[2]. Despite Forrest and Grierson's novel find, their results went unnoticed for some time. Mysels and his colleagues later observed similar behavior when they added aluminum disoaps to a gasoline stream. Their results suggested a smaller pressure drop for the gasoline and disoap stream when compared to a pure gasoline stream at the same flow rate[3]. Toms completed early studies using high molecular weight poly(methyl methacrylate) in monochlorobenzene. He observed increased flowrates under a constant pressure gradient with the addition of the polymer[4]. Due to his contributions, the "Toms Effect" is sometimes used synonymously with drag reduction[1]. Since these early discoveries, much work has been done in this field and many new additives have been found and studied extensively. The two main types of additives that are often studied are polymers and surfactants.

2.2 Polymer Drag Reduction

With the addition of high molecular weight polymer molecules in amounts as small as a few parts per million by weight, a significant reduction in turbulence can be observed. This reduction in turbulence can translate to a reduction in pressure loss approaching 90% compared to the solvent [1]. Many researchers believe that this is a result of the polymer's elongational viscosity [5]. When these coiled polymer molecules are put under stress, they unravel and their elongational viscosity can increase by several orders of magnitude. This unique property allows the polymer to stretch along the pipe wall affecting the turbulent boundary layer [5]. This stretching is believed to cause an increase in viscosity at the wall which reduces the propagation of turbulent eddies and turbulent energy dissipation [1]. Two of the most common water-soluble polymers that have grown in popularity due to their high cost effectiveness are polyethylene oxide and polyacrylamide [5]. Drag reduction by polymers has been utilized in a number of fields including fire fighting, crude oil transport, and jet cutting [6]. One large drawback to using polymers to induce drag reduction is their sensitivity to large shear stress such as those caused by a pump. These forces can destroy the polymer chains rendering them useless and eliminating any possibility of drag reduction [1]. Despite this setback, polymer induced drag reduction has found much success in many different applications. Most notably, a tremendous increase in throughput was observed in the Alyeska oil pipeline and many others. The addition of 5 to 25 ppm of a polymer material resulted in an increase of 500000 barrels of crude oil per day in this pipeline [1].

2.3 Surfactant Drag Reduction

2.3.1 Surfactant Structure

Water-soluble surfactants are comprised of two parts. The first is a hydrophilic head group and the second is a hydrophobic tail. The tail is typically composed of a long hydrocarbon chain. Tail lengths can vary anywhere from six to eighteen carbons in length. Under the right conditions, surfactant monomers can aggregate into larger structures called micelles[1]. Formation of micelle structures is largely dependent on temperature and concentration. When the concentration of a surfactant in a solution exceeds its critical micelle concentration (CMC) micelles can form if the temperature of the system is above the critical micelle temperature or Krafft temperature[1]. Above the CMC these structures are in thermodynamic equilibrium with the monomer molecules[1]. Micelles form by reorienting the surfactant molecules so that the hydrophobic tails align themselves on the inside while the head groups align on the outer edges. This process sequesters the sufactant tails away from the aqueous solution and keeps the hydrophillic heads in contact with the water phase along the outer edges of the micelle[1]. As the concentration continues to increase beyond the second critical micelle concentration, rod-like micelles will form instead of spherical ones. This process can be seen in Figure 1.

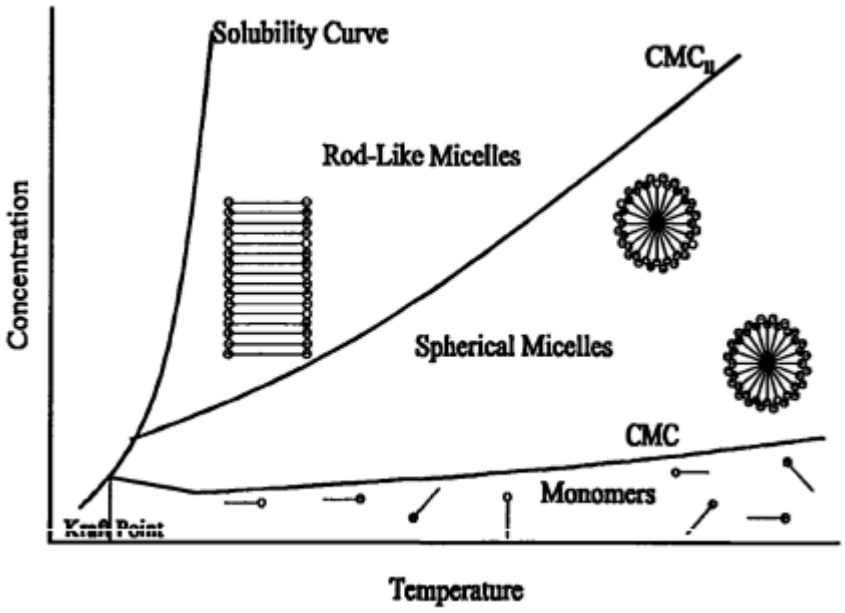

Figure 1: Surfactant phase diagram [1]

The self-assembled micelles can break apart and reassemble when subjected to high shear. This re-assembly process can take place on the order of a few seconds [1]. This unique ability is one reason why surfactants have attracted much attention in various industries. Furthermore, this advantage sets them apart from polymer drag-reducing additives which undergo irreversible shear-induced degradation [7].

2.3.2 Types of Surfactants

Surfactants are generally classified under two groups depending on the charge, or lack of charge, that the head group carries. Ionic surfactants feature a charged head group and can be further categorized depending on the sign of the charge [8].

Cationics carry a positive charge while anionics carry a negative charge[8]. Non-ionic surfactants, the second class of surfactants, are of three different types. Zwitterionics feature both a cationic and an anionic group attached to the head[8]. Semipolar and single-bond make up the two remaining types of non-ionics. The system that we will be discussing is comprised of a cationic mixed with a zwitterionic. In addition to surfactants, these systems are often stabilized with a counterion. The counterion aids in the process of micelle formation by neutralizing electrostatic repulsion[8]. For our study, we used sodium salicylate.

2.3.3 Surfactant Mechanism of Drag Reduction

The mechanism by which surfactant drag reduction occurs, although studied extensively, is still rather poorly understood. It was believed that this phenomenon shared a cause similar to that of polymer systems namely, the elongational viscosity property[7]. This belief has since been brought into question with the observation that drag reduction is able to occur in systems with a small elongational viscosity[7]. An important characteristic of drag reduced flow is the presence of wormlike micelles. These micelles are long, threadlike, self-assembled structures[7]. They have a diameter twice the length of a single surfactant monomer and can reach tremendous lengths. Lengths can reach thousands of times the molecular size[7]. The presence of these micelles can greatly alter flow behavior and significantly reduce turbulent pressure losses.

One hypothesis which has grown in popularity is the idea of an effective wall slip. Under turbulent flow, the high shear forces can induce the formation

of a gel in the turbulent boundary layer near the pipe wall[7]. This gel coats the wall and greatly reduces the friction experienced by the fluid. As a result, energy dissipation is significantly reduced and a much smaller pressure drop is observed[7]. The presence of a shear-induced gel can be observed in Figure 2.

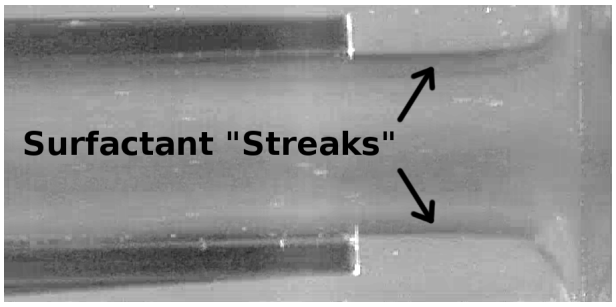

Figure 2: Streaks in DR flow[9]

2.4 Dilution Precipitation

Dilution precipitation is a rather unique and rare phenomenon. A stable aqueous solution can suddenly become two phased with a small addition of solvent. In the case of our drag reducing solution, the addition of water produces a white, globular precipitate that settles at the top of the solution. The size and compactness can vary depending on relative amounts of each surfactant and this is something we set out to explore and quantify. This phenomenon was first observed in our system using a solution consisting of equal molar parts of a zwitterionic surfactant and a cationic surfactant at a total concentration of 7.5 millimolar. Sodium salicylate was used as a counterion at a molar ratio of 1.33:1, sodium salicylate to total surfactant. Upon 100% dilution to a new

concentration of 3.75 millimolar, a precipitate was observed. The precipitate can be seen in Figure 3.

Figure 3: Precipitated DR fluid

Kato observed a similar result where certain concentrations of a mixed cationic and anionic solution resulted in the formation of a precipitate[10]. In his paper, a partial phase diagram was constructed which plotted a precipitous region that primarily existed at cationic concentrations near the equimolar line and greater[10]. Kato's phase diagram is show in Figure 4. Total surfactant concentration is plotted on the y-axis while mole fraction of octyltrimethylammonium bromide (OTAB), the cationic surfactant, is shown on the x-axis. The region labeled "P" represents a region where precipitation occurs while the "M" region is one where micellar, one phase behavior exists. The "S" denotes a region where surfactant monomers exist.

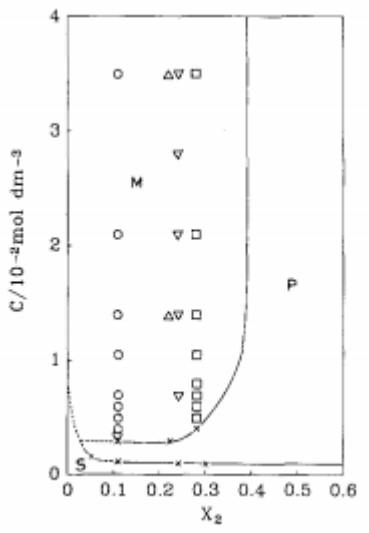

Figure 4: Partial Phase Diagram (Total Surfactant Concentration vs. Mole Fraction of OTAB)[10]

Although Kato's results were based on a mixed cationic and anionic system, whereas our system is a mixed zwitterionic and cationic system, we expected the precipitous regions to be similar. In a similar fashion, Kaler et al. showed that vesicles, which were in equilibrium with the lamellar phase at high concentrations, could be precipitated out upon dilution to a lower concentration[11]. Their region of precipitation also occurred near the equimolar line. As a result, in producing our phase diagram, solutions were prepared near the equimolar line and extended to the right of it at greater concentrations of the zwitterionic surfactant. Preliminary phase diagrams can be seen in Section 4.1.

2.5 District Heating and Cooling

One attractive application of drag reducing surfactant solutions is to use them in district heating and cooling systems (DHCS). Such systems would allow for the fluid to be heated or cooled at a central location and then pumped through a city district or neighborhood providing cooling relief during the summer or much needed heat during the winter months[8]. These systems are commonly used in several European countries, China, and Japan. They have been shown to be highly effective. In one study conducted by Matthys and his colleagues, a 30% pumping power savings was achieved when surfactants were employed in a DHCS system in a medium sized building[12]. Despite the reduction in pumping power requirements, there is a serious drawback. This drawback is the reduced heat transfer ability of these systems. This occurs due to a decrease in convective heat transfer coefficients caused by the reduction in radial turbulence[8].

Various methods of improvement have been explored to enhance the heat transfer ability of these solutions. Some induce turbulence by forcing fluid flow through cavities or channels causing the reversible break up of the micelles resulting in more water-like behavior[8]. Examples include static mixers, wire mesh, active mixers, and impinging jets. Others utilize less invasive means to break up the micelles. These include ultraviolet radiation and ultrasonic energy. Regardless of the method, the objective is the same. Thus, imparting energy into the fluid, the goal is to break apart the micelle structures to return the fluid to its solvent properties to facilitate improved transfer of heat[8].

2.6 Research Significance

The system we are studying, if used in a district heating and cooling system (DHCS), has a very unique characteristic that makes it desirable for this application. At certain surfactant concentrations the system is stable, drag reducing, and viscoelastic. However, if the solution is diluted, the surfactants and counterion precipitate out of solution and can be separated with relative ease. This is useful in that it allows for a cheap separation that requires no additional energy input to the system. Theoretically, this would allow a DHCS operator to replace the drag reducing solvent while recycling the drag reducing components namely, the surfactants and counterion. Furthermore, this would allow for an easy removal of biological contaminants, dissolved metal ions, and any other foreign materials which may cause fouling. Since the solvent is water, this is a very cost-effective technique to maintain a DHCS system. Furthermore, in the case that a system is to be brought offline and the DHCS fluid needs to be disposed of, this separation can be employed to safely separate the materials so that they may be dealt with properly. This would mitigate potential damages to the environment that may be caused by the unsafe release of these materials and would reduce waste treatment costs.

3 Materials and Methods

Two different surfactants were used in this study. The first is 3-(N,N-Dimethylpalmitylammonio) propanesulfonate, a zwitterionic surfactant from Fluka chem-

icals. It has a molecular weight of 391.66 g/mol and a purity of greater than 99%. It is commonly known as SB3-16 or zwittergent 3-16. SB3-16's structure is shown below in Figure 5.

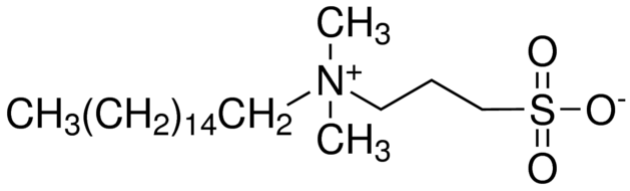

Figure 5: SB3-16 Chemical Structure

The second surfactant used is Arquad S-50 (Soya-N$(CH_3)_3$Cl). It is a cationic surfactant and it's also a quaternary ammonium salt. S-50 is sold as a distribution of hydrocarbon chain lengths. C18 chains comprise approximately 81% of the product and C16 chains make up 17%[13]. Of the total chains, 70% are unsaturated. This surfactant is produced by Akzo-Nobel, formerly Akzo Chemical. It is typically sold mixed with an isopropanol solvent at 50% by weight. It was later experimentally determined that, due to the age of our supply, evaporation had reduced the isopropanol content to just 20%. This was taken into consideration when samples were being made. S-50 has a mean molecular weight of 430.00 g/mol. Its structure is shown in Figure 6.

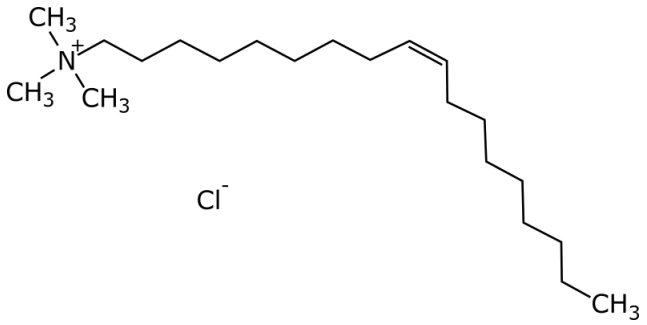

Figure 6: S-50 Chemical Structure

The last component used is sodium salicylate (NaSal). NaSal was obtained from Sigma-Aldrich and acts as the counterion for this system. It has a molecular weight of 160.11 g/mol and is a white, crystalline solid. The structure of NaSal is shown in Figure 7.

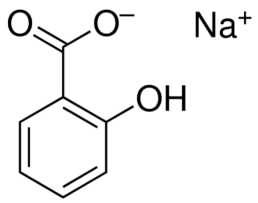

Figure 7: NaSal Chemical Structure

3.1 Phase Characterization

In order to properly characterize this system, an understanding of phase behavior is needed. For this to be accomplished, it was necessary to prepare many samples to determine under what conditions precipitation occurs. A partial factorial experimental design was produced for an early exploration of the de-

sign space. This was done using JMP, a statistical analysis software package developed by SAS Institute. This design consisted of 36 samples of different compositions randomly selected by the program. Three parameters were varied in this design. The first is the mole fraction of SB3-16 compared to the moles of total surfactant. Five different fractions were considered. These were 0.125, 0.25, 0.5, 0.75, and 0.875. Calculation of the mole fraction was done by using Equation 1, shown below. The second parameter was the total concentration of surfactants in the system. This parameter was tested at four different concentrations. These were 3.75, 5, 6.25, and 7.5 millimolar. Using equation 2, total concentration was calculated. The final parameter that was varied was the counterion ratio. Four different ratios were tested. These include 1:1, 1.16:1, 1.33:1, and 1.5:1 where the first number represents the relative molar amount of NaSal and the second number represents the total relative molar amount of surfactant. Calculation of the counterion ratio was done using Equation 3. In these equations, x denotes mole fraction of a particular species, n represents number of moles, and V represents volume of solvent.

$$x_{SB3-16} = \frac{n_{SB3-16}}{n_{SB3-16} + n_{S-50}} \tag{1}$$

$$C_{total} = \frac{n_{SB3-16} + n_{S-50}}{V_{water}} \tag{2}$$

$$NaSal_{ratio} = \frac{n_{NaSal}}{n_{SB3-16} + n_{S-50}} \tag{3}$$

To facilitate easier production of samples, stock solutions of each component were mixed. The S-50 stock was produced by mixing 0.6047 grams of S-50 in 50 milliliters of research grade water. A solution of 0.7956 grams of SB3-16 mixed with 100 milliliters of research grade water was also prepared. Due to the inability of the SB3-16 to dissolve in water, 0.6000 grams of sodium salicylate was added. The third stock contained 0.6004 grams of sodium salicylate dissolved in 50 milliliters of research grade water.

With the stock solutions prepared, a micropipette was used to dispense the proper amount of each component into 36 five milliliter vials. Each vial was sealed with parafilm and allowed to equilibrate over a 48 hour period before being analyzed. Based upon the results of the initial 36 vial screening, an additional 36 vials were prepared. Each of these vials was then divided into four additional vials. Each of the four vials was filled with one milliliter from the parent vial and subsequent dilutions were carried out over the following weeks. Each of these vials were also wrapped with parafilm to minimize moisture loss due to evaporation to ensure accurate data collection. A photo of the 144 child vials and the 36 parent vials are shown below in Figure 8

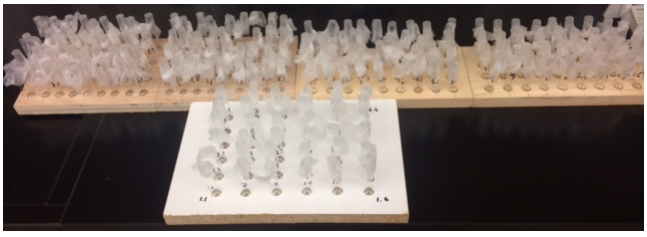

Figure 8: Prepared Samples

3.2 Precipitate and Supernatant Identification

An equimolar solution at a total surfactant concentration of 7.5 millimolar was prepared. A five milliliter sample was diluted with five milliliters of research grade water. Upon dilution of the drag reducing (DR) fluid, a solid precipitated out of the solution. Separation of the precipitate from the remaining liquid was carried out. The larger chunks of precipitate were collected in a petri dish after being scooped out of the liquid. The precipitate was set aside and allowed to dry in a fume hood. The remaining liquid was poured through a funnel and trace amounts of precipitate were collected in the filter paper. The filtered supernatant was collected in a vial for later testing.

Identification of the dried precipitate and supernatant components was attempted using infrared spectroscopy. A Thermo Nicolet Magna-IR 550 was used to examine samples. Scans were performed of the principal components, the DR fluid, the dried precipitate, and the supernatant.

3.3 Drag Reduction Experiments

Evaluation of drag reduction properties of our fluid was carried out using a recirculating system show in Figure 9. This system is 36 feet in length and consists of several components.

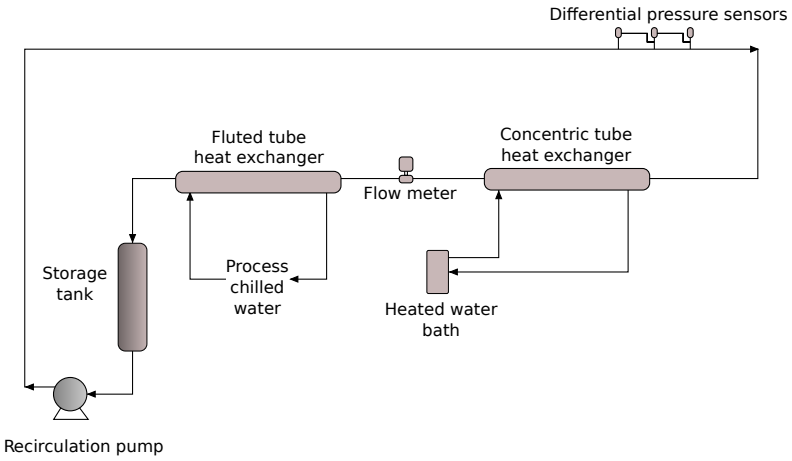

Figure 9: Recirculating System

A 10 liter storage tank is used to store the drag reducing fluid. A 2 horsepower gear pump provides the driving force to pump the solution through the system. Two Omega PX2300 differential pressure sensors are used to evaluate the pressure drop experienced by the fluid. These work by generating an electrical signal depending on the magnitude of the pressure difference. This signal is sent to a DaqBoard 2000 data acquisition board which then outputs the signal to a spreadsheet on the computer where it can be interpreted. The fluid then travels to a concentric tube heat exchanger. However, due to time constraints, heat transfer enhancement was not studied. Therefore, this section of the system merely acts as a straight tube section of pipe. At the outlet of the concentric heat exchanger, a Toshiba LF404 electromagnetic flowmeter is used to measure the volumetric flow rate. This flow meter works by electromagnetic induction. A magnetic field is applied and the potential difference is measured which is proportional to the flow rate. A flow rate is then output to the screen

of the flowmeter. The fluid then flows through a fluted tube heat exchanger which uses process chilled water from the East Regional Chilled Water Plant. The purpose of this exchanger is to remove heat from the fluid that develops as a result of viscous heat dissipation. The fluid then returns to the storage tank. In addition to the components mentioned above, type T thermocouples are used to monitor the fluid temperature during the experimental trials. These produce an electrical signal based on the magnitude of the temperature which is then interpreted by a Physitemp Bat-10 multipurpose thermometer. The resulting system temperature is shown on the Bat-10 screen.

3.3.1 Calibration of Recirculating System

Prior to gathering any data, the recirculating system required calibration. This is done by first completely emptying the system. Next, the system must be rinsed by adding several liters of water, recirculating the water, and then emptying the system again. This is done at least three times to ensure that any trace amounts of other components are completely flushed out. The tank is then filled with eight liters of pure research grade water. With the pump off, a data point is taken from the differential pressure sensors to represent zero differential pressure. Next, the pump is turned on and adjusted to a known flow rate. Using this flow rate and the cross-sectional area of the pipe, a linear velocity is calculated using Equation 4.

$$u = \frac{Q}{A} \tag{4}$$

Density and viscosity values are obtained from literature based upon the temperature of the water and are used with the pipe diameter and calculated linear velocity to calculate the Reynolds Number. This is done using Equation 5.

$$Re = \frac{\rho u D}{\mu} \tag{5}$$

After calculating the Reynolds number, an iterative solution can be obtained for the fanning friction factor. This is done using the Von Kármán equation, Equation 6.

$$\frac{1}{\sqrt{f}} = 0.86 ln(Re\sqrt{f}) - 0.8 \tag{6}$$

Pressure drop can then be calculated by using the fanning friction factor, pipe length and radius, density, linear velocity, and Equation 7.

$$\Delta P = f \frac{L}{R} \rho u^2 \tag{7}$$

Once the pressure drop is known for this flow rate, a plot can be made of pressure drop versus voltage signal. A linear trendline can be drawn and the resulting line equation can be used to interpolate pressure drop values for a given voltage signal. This can be done because the output of the differential pressure sensors is linear with pressure drop.

3.3.2 Preparation of Drag Reducing Fluid

Twelve liters of DR solution were prepared for the drag reduction trials. This batch was made by mixing 19.9750 grams of SB3-16, 29.6700 grams of S-50, 19.2134 grams of NaSal, and twelve liters of research grade water. This gives a SB3-16 mole fraction of 0.425 and a counterion ratio of 1:1. A Cole-Parmer Polystat immersion circulator was used to mix and heat the solution to ensure solubility of the components. Two liters were then added to the system and allowed to circulate. This was done to ensure that excess water left behind would be removed. The system was then emptied again and refilled with the remaining ten liters. Upon collection of the first few data points, it was observed that the effect of drag reduction was rapidly decreasing to zero. Shear forces had caused the DR fluid to precipitate. To remedy this, the tank was emptied and the counterion ratio was modified. An additional 5.2838 grams of NaSal was added to increase the ratio to 1.33:1. The immersion circulator was used again to mix and equilibrate the solution. Once well mixed, the fluid was added back to the tank and data were ready to be collected. Testing over a range of solvent Reynolds numbers, pressure drop readings were collected and friction factors were calculated along with DR percentage.

3.4 Rheological Experiments

Drag reducing fluids belong to a class of fluids known as viscoelastic fluids. These fluids are often classified as being non-Newtonian because their viscosities exhibit a nonlinear dependence on the strain rate, unlike Newtonian fluids [14].

Viscoelastic fluids exhibit properties found in both elastic solids and viscous liquids[14]. One important property of these fluids is known as the first normal stress difference. In Newtonian fluids, this force is zero however, in non-Newtonian fluids, this force can vary greatly in magnitude and acts as a measure of viscoelasticity. As a viscoelastic material is sheared, a force is generated that acts perpendicularly to the direction of shear[14]. This property is directly responsible for a phenomenon known as the Weissenberg effect, or more commonly known as the rod climbing effect. An example of this is shown in Figure 10. A large first normal stress difference is important for drag reducing fluids because it is generally associated with better DR performance.

Figure 10: Weissenberg Effect[14]

A TA Instruments Ares rheometer was used to measure viscoelastic properties. The 50 mm cone and plate fixture was used as this is the best geometry to study the presence of a first normal stress difference. This fixture has a 0.02 radian cone angle and was used at a gap setting of 0.0559 mm. A maximum

shear rate of 1000 reciprocal seconds was used. Measurements were taken for the DR solution, the supernatant, and a solution that had been reconstituted to determine how the presence and strength of the first normal stress difference is correlated with the drag reducing effectiveness of the fluid. The reconstituted solution was made by collecting the precipitate and dissolving it in fresh solvent of the original volume.

4 Results and Discussion

4.1 Phase Characterization

Using the results of the initial screening trial, four phase diagrams were created. One diagram was produced for each counterion ratio. In each diagram, the black dots represent the concentrations tested during the preliminary screening process. The grey shaded regions represent a hypothesized region where precipitous behavior exists. Dots that appear within these shaded regions are samples which precipitated. The phase diagrams representing the 1:1, 1.166:1, 1.33:1, and 1.5:1 counterion ratios are shown below in Figures 11, 12, 13, 14, respectively. In these diagrams, C represents mole fraction of water, B represents mole fraction of SB3-16, and A represents mole fraction of S-50.

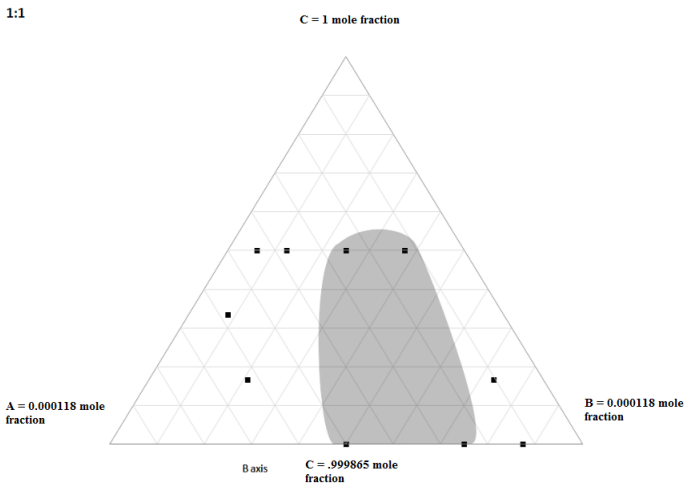

Figure 11: Preliminary Phase Diagram for 1:1 Counterion Ratio

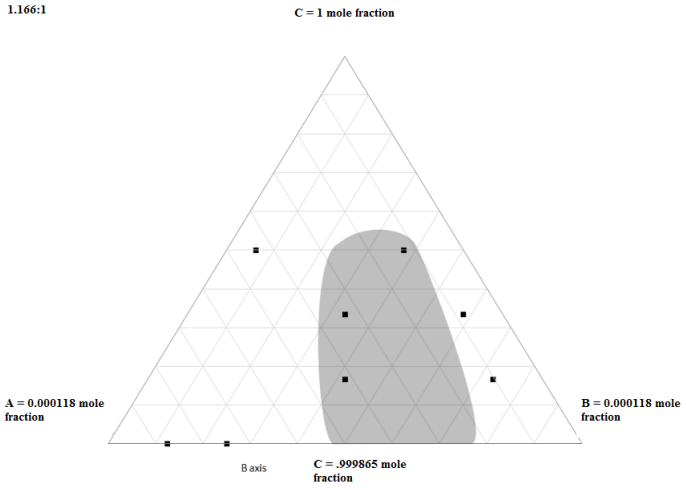

Figure 12: Preliminary Phase Diagram for 1.166:1 Counterion Ratio

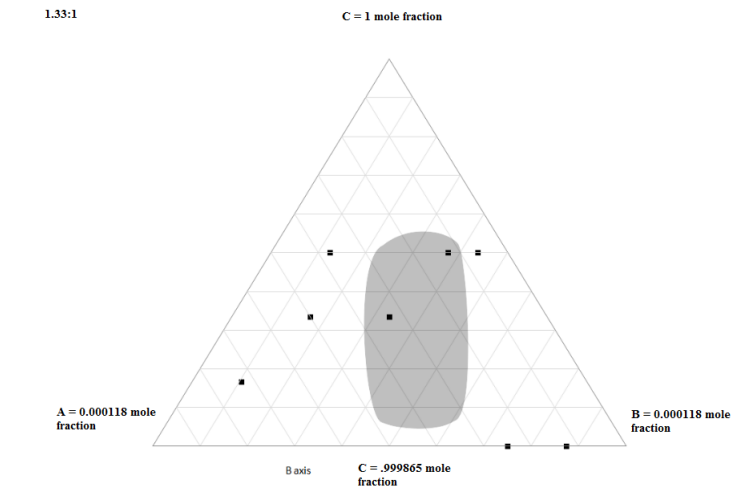

Figure 13: Preliminary Phase Diagram for 1.33:1 Counterion Ratio

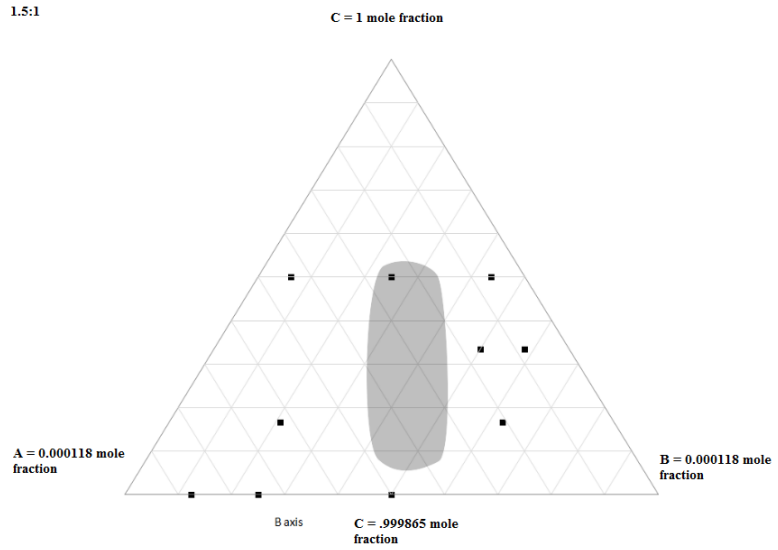

Figure 14: Preliminary Phase Diagram for 1.5:1 Counterion Ratio

Based on these results, it was observed that precipitation occurs at greater total surfactant concentrations when the counterion ratio is smaller. It was

hypothesized that in addition to a shrinking precipitous region at lower counterion ratios that this window would also get narrower. Last, precipitation did not occur in any of the vials when SB3-16 made up less than half of the total surfactant concentration. This finding reinforced an earlier stated hypothesis in Section 2.4 that precipitation would likely not occur in systems where SB3-16 was not at equimolar concentration with S-50. Based on these observations and assumptions, the grey shaded regions were drawn.

Following the initial screening, 36 more vials were produced using the stock solutions described in Section 3.1. Nine vials were prepared for each counterion ratio at SB3-16 mol fraction percentages spanning 0.4375 to 0.8125. Each of these parent vials were produced at a total surfactant concentration of ten millimolar and a total volume of five milliliters. This concentration was chosen to ensure solubility prior to the dilution trials. Each parent vial was then divided into four child vials. One milliliter from the parent vial was dispensed into each of the child vials. The child vials were then diluted using research grade water and a micropipette. Dilutions were performed to reach concentrations of 9.75, 9.5, 9.25, and 9 millimolar. After allowing samples to equilibrate they were analyzed and recorded based on the presence or lack of presence of a precipitate. Dilutions were again performed to obtain new concentrations of 8.75, 8.5, 8.25, and 8 millimolar. This process was repeated until 0.75 millimolar was reached. The results of these trials are show in the phase diagrams shown in Figures 15, 16, 17, and 18. These diagrams represent 1:1, 1.166:1, 1.33:1, and 1.5:1 counterion ratios, respectively.

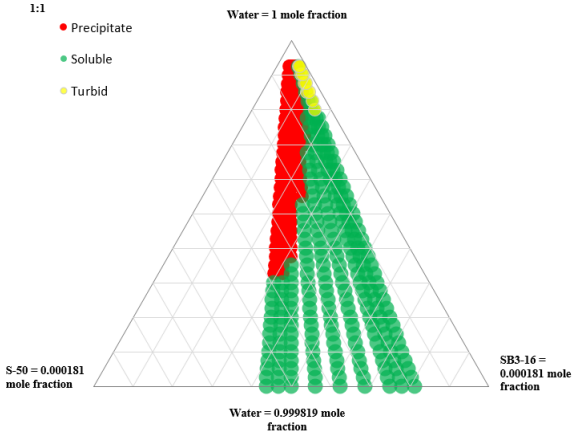

Figure 15: Phase diagram for 1:1 counterion ratio

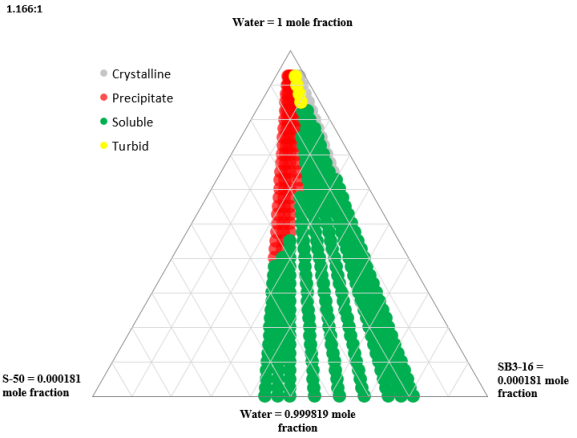

Figure 16: Phase diagram for 1.16:1 counterion ratio

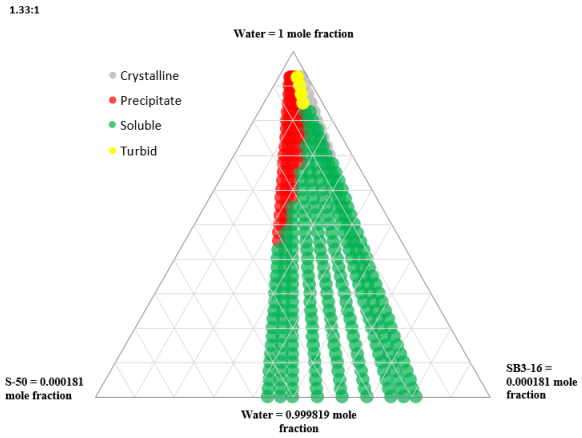

Figure 17: Phase diagram for 1.33:1 counterion ratio

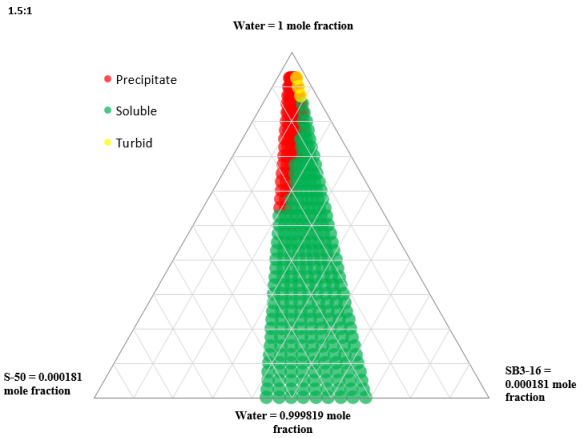

Figure 18: Phase diagram for 1.5:1 counterion ratio

In general, our hypotheses were correct. At lower counterion ratios, the window of precipitation is much larger and precipitation occurs at greater concentrations. When the counterion ratio is increased, the region of precipitation shrinks and the system is more stable at more dilute concentrations. One interesting finding is that precipitation can occur to the left of the equimolar line;

that is, in systems where SB3-16 makes up less than half of the total surfactant concentration. This finding prompted us to explore further in order to locate the center of the precipitous region. This is the point at which precipitation can occur at the greatest total surfactant concentration. This was found to be at an SB3-16 mole fraction of 0.4.

Another unique finding was that at an SB3-16 mole fraction of 0.75, a new type of precipitate is observed. This precipitate is very different from the white, globular precipitate previously seen in Figure 3. This precipitate is a clear, crystalline precipitate. Presumably, this precipitate has its own unique region of precipitation that occurs at and beyond an SB3-16 mole fraction of 0.75. This precipitate can be seen in Figure 19.

Figure 19: Crystalline Precipitate

4.2 Precipitate and Supernatant Identification

An equimolar solution at a concentration of 7.5 millimolar was diluted to a concentration of 3.75 millimolar. The sample precipitated and a separation was carried out. The precipitate was isolated in a petri dish and the supernatant was poured through a funnel and filter paper. The supernatant was collected in a vial.

Infrared spectroscopy was used to identify precipitate and supernatant components. Initial scans were performed on SB3-16, S-50, and NaSal to identify characteristic peaks that could be identified in the precipitate and supernatant. The results of these scans are shown in Figures 20, 21, and 22, respectively.

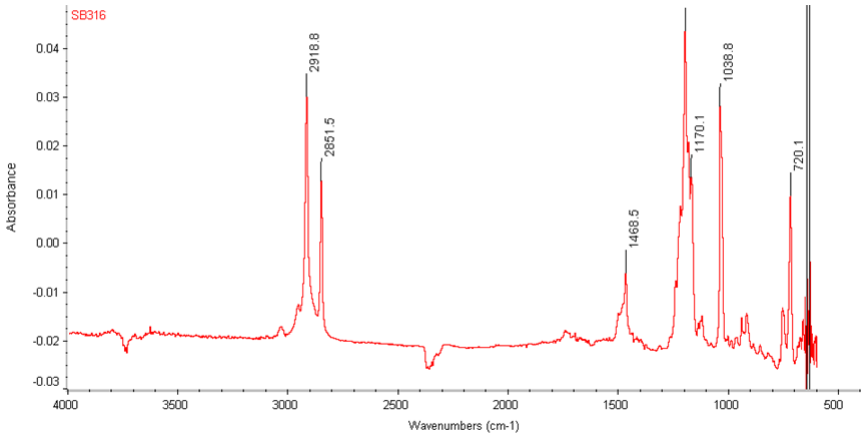

Figure 20: Infrared spectrum of SB3-16

There are several peaks which are significant for the SB3-16 component. Specifically, the peaks at 2918.8, 2851.5, 1038.8 and 721.1 cm^{-1}. These peaks are unique and should be looked for in the precipitate and supernatant scans.

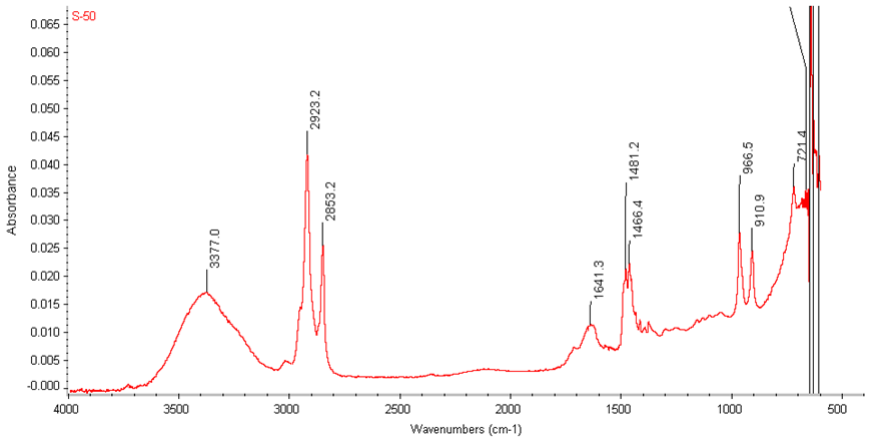

Figure 21: Infrared spectrum of S-50

The S-50 scan has many significant peaks but is complicated by the fact that the surfactant is mixed with isopropanol which produces it own unique peaks. For instance the wide peak at 3370 cm^{-1} is due to the isopropanol. Furthermore, the significant peaks of S-50 are often similar to the SB3-16. As a result, it will be difficult to distinguish these two using infrared spectroscopy. Regardless, the important peaks to consider are at 2923.3, 2853.2, 1466.4 cm^{-1}.

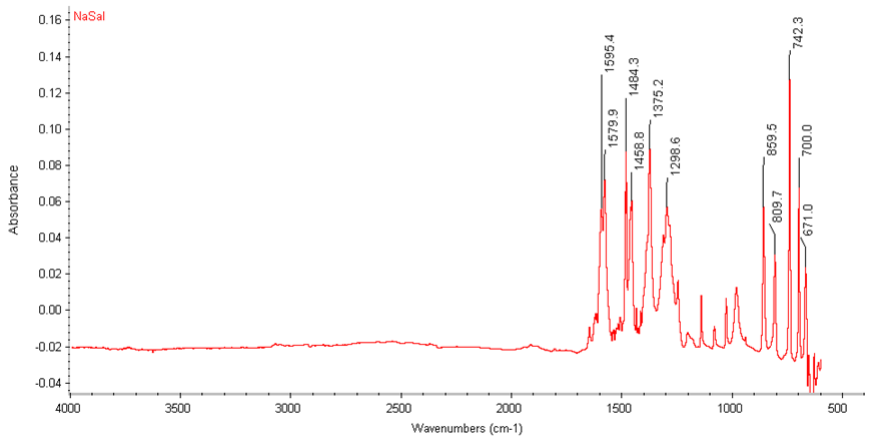

Figure 22: Infrared spectrum of NaSal

NaSal has several distinctive peaks that occur. Specifically, the peaks at 859.5, 1375.2, and 1484.3 cm^{-1}.

After performing scans of the principal components, the precipitate was separated from the supernatant and was dried in a fume hood using a hot plate to accelerate evaporation of residual moisture. Once sufficiently dried, a scan of the precipitate was performed. The spectrum for the dried precipitate is shown in Figure 23.

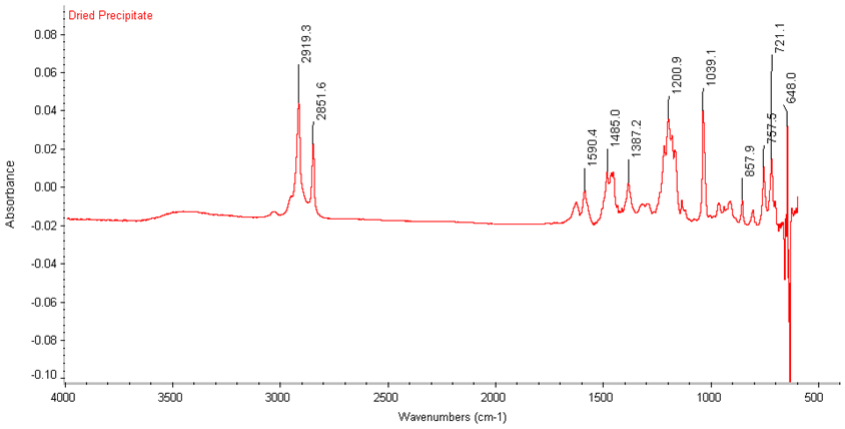

Figure 23: Infrared spectrum of dried precipitate

The precipitate resulted in large peaks at 2919.3 and 2851.6 cm^{-1}. These most likely occurred due to the presence of each surfactant. Additional peaks were observed at 1039.1 and 721.1 cm^{-1} which are very close to peaks observed for SB3-16 which saw peaks at 1038.8 and 721.1 cm^{-1}. Last, peaks were observed at 857.9, 1387.2, and 1485.0 cm^{-1}. These are very close to the peaks observed for NaSal at 859.5, 1375.2, and 1484.3 cm^{-1}. It seems that the precipitate contains all three of the principal components.

A scan was also performed on the supernatant after the precipitate was removed and it was poured through a funnel and filter paper. The resulting scan is shown in Figure 24.

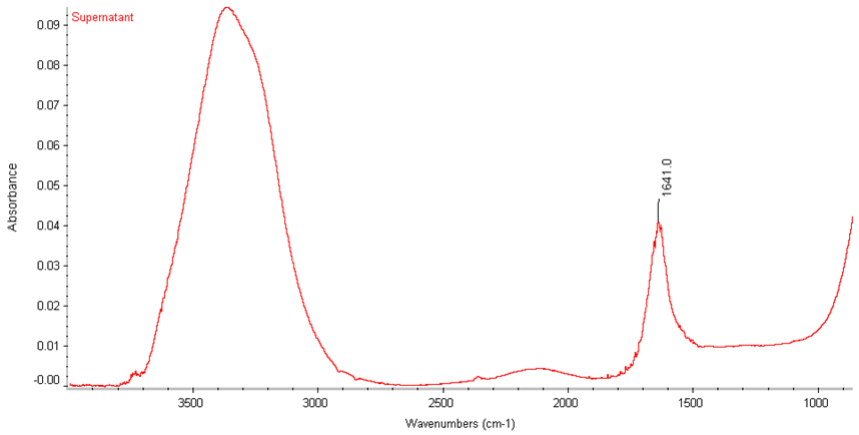

Figure 24: Infrared spectrum of supernatant

The supernatant doesn't contain any of the peaks mentioned above. Furthermore, it looks very similar to the scan of pure research grade water which is shown below, Figure 25. If the supernatant does contain any of the three components, it is probably at concentrations so low that infrared spectroscopy will not be able to observe them.

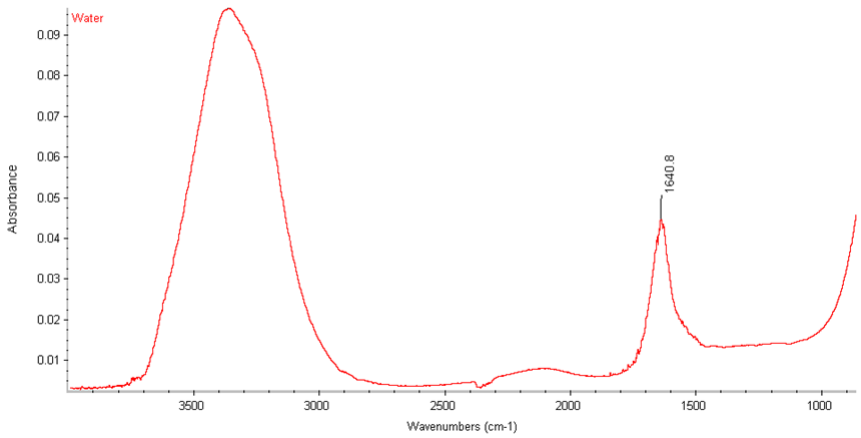

Figure 25: Infrared spectrum of research grade water

4.3 Drag Reduction

Data were collected over the range of 10000 to 40000 Reynolds Number for research grade water and for a batch of DR fluid. As stated in Section 3.3.2, twelve liters of DR fluid was prepared at a 0.425 mole percentage of SB3-16 and at a total concentration of eight millimolar. The solution was initially prepared at a counterion ratio of 1:1 but was modified to 1.33:1 after shear precipitation was observed.

Over this range of Reynolds numbers, the friction factor at a given flow rate is compared for water and for the DR fluid. Values for water are obtained by using the Von Kármán equation that was described in Section 3.3.1. Values for the DR fluid are experimentally determined using the pressure drop observed by the pressure sensors. The percent drag reduction is computed using Equation 8.

$$\%DR = \frac{f_{water} - f_{DR}}{f_{water}} \tag{8}$$

The results of the drag reduction trial are shown in Figure 26.

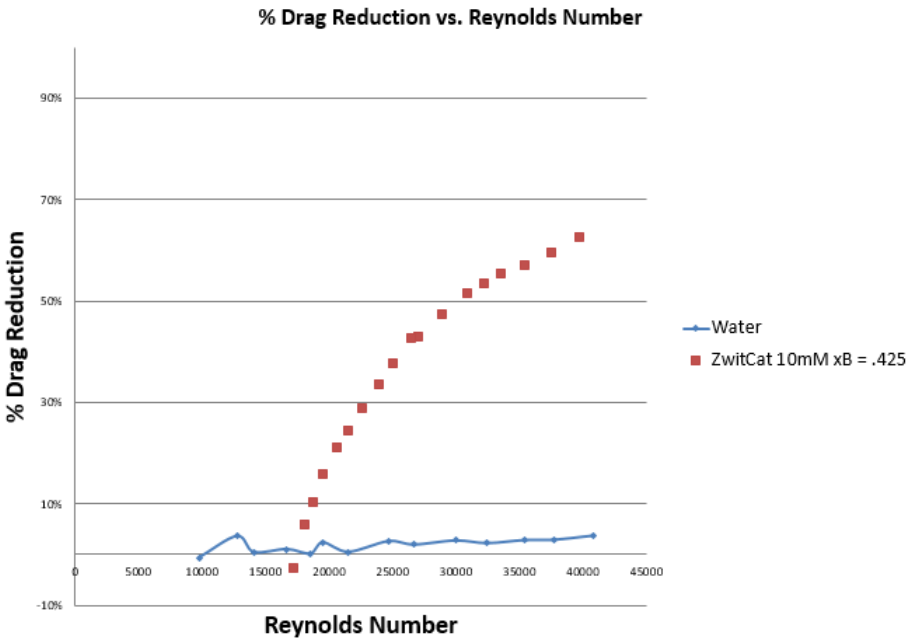

Figure 26: Drag reduction data

The DR fluid is a very effective drag reducer at higher flow rates. At approximately 17500 Reynolds Number the DR percentage is zero. Below this Reynolds Number, the pump actually would need to work harder to pump the DR fluid when compared to water. Above this value, the work required steadily decreases. Assuming this trend continues, at flow rates in excess of 40000, the DR percentage will continue to increase. This solution is a very effective drag reducer.

4.4 Rheology

Rheology data were collected for the regular solution, the supernatant, and a reconstituted solution. The reconstituted solution was made by collecting the precipitate from a diluted solution, allowing it to dry, and then dissolving the precipitate in its original volume of research grade water. The results for the drag reducing solution are shown in Figure 27.

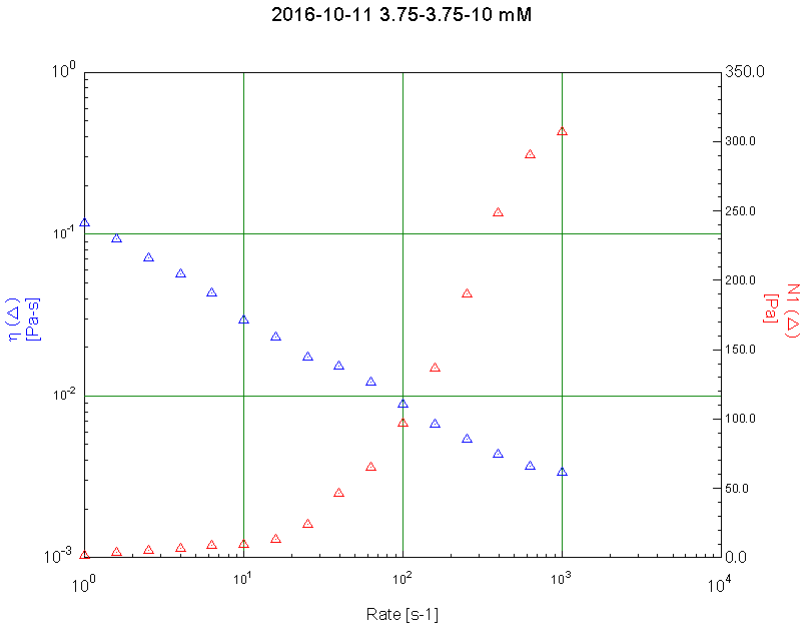

Figure 27: Rheological behavior of 10 millimolar equimolar solution

The DR fluid being tested was made at a concentration of 10 millimolar in equimolar ratios of SB3-16 and S-50. It also contains sodium salicylate at a ratio of 1.33:1. This fluid is highly viscoelastic which can be seen by the rapid growth of the first normal stress difference (N1). Furthermore, it is a shear

thinning fluid because its viscosity rapidly decreases as shear rate is increased. Due to the large N1 observed, it can be expected that this solution will be an effective drag reducer.

After diluting this sample, the precipitate was removed and the remaining fluid was poured through a funnel and filter paper. The supernatant, was tested under the same conditions. Results can be seen in Figure 28.

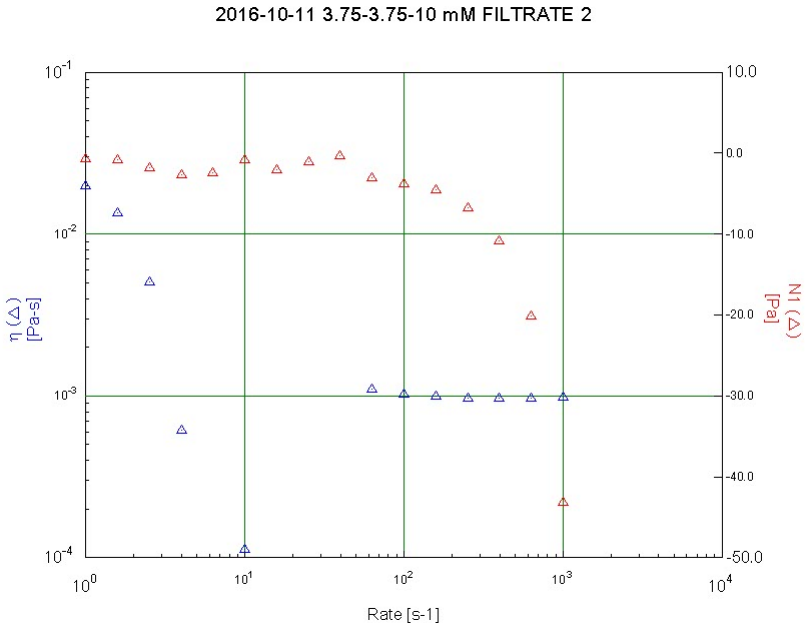

Figure 28: Rheological behavior of 10 millimolar equimolar supernatant

The supernatant shows no generation of N1. Its viscosity begins to fall but then steadies around a value of 0.001 Pa*s, the viscosity of water. This fluid demonstrates very normal, Newtonian behavior and it's expected that it would be a very poor drag reducer. It's very likely that the supernatant is mainly

water with trace amounts of some of the drag reducing components.

After isolating the precipitate and drying it, it was dissolved in a beaker with the original amount of water. Once it was sufficiently re-dissolved, it was tested under the same conditions as the previous two tests. Figure 29 shows the results of this measurement.

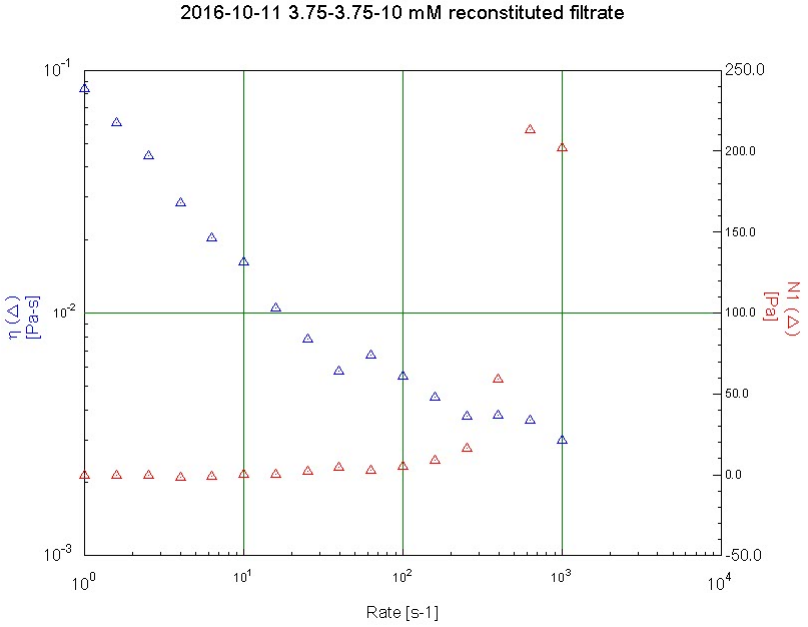

Figure 29: Rheological behavior of reconstituted drag reducing solution

The reconstituted solution shows that viscoelastic properties have been recovered. As shear rate increases, the N1 tends to increase too. The fluid has become shear thinning again which is shown by the decreasing viscosity with increasing shear rate. It appears that the reconstituted solution would be an effective drag reducing fluid. It is interesting to note however, that only approximately 67% of the N1 has been recovered.

5 Conclusion

5.1 Recommendations and Future Work

5.1.1 Heat Transfer Enhancement

Due to time constraints, heat transfer enhancement was not explored for this DR fluid. It would be interesting to see how temperature affects the drag reduction percentage. Furthermore, trials should be performed using the various methods of heat transfer enhancement mentioned in Section 2.5. These include static mixers, active mixers, and many others. Doing so would allow us to evaluate the effectiveness of these methods on this particular DR fluid.

Because this system provides many options based on the varying concentrations of the three components, many more trials of drag reduction and heat transfer enhancement should be tested. A more extensive exploration of these variables would be valuable to see how things such as counterion ratio, mole fraction, total surfactant concentration, and temperature affect drag reduction and heat transfer. This was not possible during this study because of material limitations and time constraints.

The unusual behavior of this fluid is that it exhibits shear precipitation. This was observed during drag reduction trials as discussed in Section 4.3 which made modification of the counterion ratio necessary. We learned that when the solute precipitates, the residual fluid has no drag reducing effectiveness and behaves like water. If the conditions under which shear precipitation occurs were better understood, a solution could be produced that prior to entering a

heat exchanger could be subjected to large shear stresses. These would cause the fluid to precipitate and allow it to regain its heat transfer ability. As heat was transferred to the system, it would drive the two phase solution back into a single phase, drag reducing fluid. If a system such as this could be perfected it would be an excellent DHCS fluid.

There are two underlying problems with this system. The first is that the time required for the precipitate to go back into solution varies for different concentrations and at different temperatures. It would require a thorough exploration of these conditions to determine the practicality of this system. Second, the shear stress required to cause precipitation varies based on surfactant concentration as well as counterion ratio. A solution would have to be found that can withstand the shear stresses during regular pumping but can precipitate when subjected to the increased shear stresses at the heat exchanger entrance.

5.1.2 Improved Recovery Methods

While separating the precipitate from the supernatant, a simple funnel and filter paper was used. Using an equimolar solution with a counterion ratio of 1.33:1, approximately 78%, by weight, of the drag reducing components were recovered. It would be beneficial to test recovery effectiveness using different mole fractions and counterion ratios to see which systems resulted in the highest recovery. Furthermore, alternate methods of separation should be explored to see if there are more efficient means of separation.

5.1.3 Conclusion

In general, it was observed that this system exhibits very interesting phase behavior. Increasing the relative amount of counterion stabilizes the system which requires further dilution to cause precipitation. While in a stable single phase form, this DR fluid is a highly effective drag reducer. If the fluid exhibits shear precipitation or dilution precipitation, all drag reduction is lost and the fluid behaves like water. More work must be done to characterize and quantify the precipitate makeup and to determine the best method of recovery. With a more complete understanding, this DR fluid could be utilized as a highly effective district heating and cooling fluid.

References

[1] Jacques L. Zakin, Bin Lu, and Hans-Werner Bewersdorff. Surfactant drag reduction. *Reviews in Chemical Engineering*, 14(4-5), 1998.

[2] F Forrest and G.A. Grierson. *Paper Trade Journal*, 92(22):39–41, 1931.

[3] K.J. Mysels. U.s. patent 2,492,173. 1949.

[4] B.A. Toms. Some observations on the flow of linear polymer solutions through straight tubes at large reynolds numbers. *in Proceedings of the 2nd International Congress on Rheology*, pages 135–138, 1948.

[5] Daniel Bonn, Yacine Amarouchène, Christian Wagner, Stéphane Douady, and Olivier Cadot. Turbulent drag reduction by polymers. *Journal of Physics: Condensed Matter*, 17(14):S1195–S1202, 2005.

[6] Gregory Ryskin. Turbulent drag reduction by polymers: A quantitative theory. *Physical Review Letters*, 59(18):2059–2062, nov 1987.

[7] J Drappier, T Divoux, Y Amarouchene, F Bertrand, S Rodts, O Cadot, J Meunier, and Daniel Bonn. Turbulent drag reduction by surfactants. *Europhysics Letters (EPL)*, 74(2):362–368, apr 2006.

[8] H. Shi, Y. Wang, W. Ge, B. Fang, J. T. Huggins, T. R. Huber, and J. L. Zakin. Enhancing heat transfer of drag-reducing surfactant solution by an HEV static mixer with low pressure drop. *Advances in Mechanical Engineering*, 3(0):315943–315943, jan 2015.

[9] Nguyen Anh Tuan and Hiroshi Mizunuma. Advection of shear-induced surfactant threads and turbulent drag reduction. *Journal of Rheology*, 57(6):1819, 2013.

[10] Tadashi Kato, Hidetomo Takeuchi, and Tsutomu Seimiya. Change in size and composition of mixed micelles with concentration in anionic/cationic surfactant solutions. *Journal of Colloid and Interface Science*, 140(1):253–257, 1990.

[11] Eric W. Kaler, Kathleen L. Herrington, A. Kamalakara Murthy, and Joseph A. N. Zasadzinski. Phase behavior and structures of mixtures of anionic and cationic surfactants. *The Journal of Physical Chemistry*, 96(16):6698–6707, aug 1992.

[12] K. Gasljevic, K. Hoyer, and E.F. Matthys. Field test of a drag-reducing surfactant additive in the hydronic cooling system of a building - phase 2: Heat transfer control. *ASME Heat Transfer Div. Publ. HTD*, 361:255–263, 1998.

[13] B Lu, X Li, J.L Zakin, and Y Talmon. A non-viscoelastic drag reducing cationic surfactant system. *Journal of Non-Newtonian Fluid Mechanics*, 71(1-2):59–72, 1997.

[14] Christopher W. Macosko. *Rheology: Principles, Measurements, and Applications*. Wiley-VCH, 1994.